Ca^{2+}/calmodulin-dependent protein kinase II regulates cardiac Na^+ channels

Stefan Wagner,[1] Nataliya Dybkova,[1] Eva C.L. Rasenack,[1] Claudius Jacobshagen,[1] Larissa Fabritz,[2] Paulus Kirchhof,[2] Sebastian K.G. Maier,[3] Tong Zhang,[4] Gerd Hasenfuss,[1] Joan Heller Brown,[4] Donald M. Bers,[5] and Lars S. Maier[1]

[1]Department of Cardiology and Pneumology, Georg-August-University Göttingen, Göttingen, Germany. [2]Department of Cardiology and Angiology, University Hospital Münster, Münster, Germany. [3]Department of Medicine I, Division of Cardiology, University of Würzburg, Würzburg, Germany. [4]Department of Pharmacology, UCSD, La Jolla, California, USA. [5]Department of Physiology, Loyola University Chicago, Chicago, Illinois, USA.

In heart failure (HF), Ca^{2+}/calmodulin kinase II (CaMKII) expression is increased. Altered Na^+ channel gating is linked to and may promote ventricular tachyarrhythmias (VTs) in HF. Calmodulin regulates Na^+ channel gating, in part perhaps via CaMKII. We investigated effects of adenovirus-mediated (acute) and Tg (chronic) overexpression of cytosolic CaMKIIδ_C on Na^+ current (I_{Na}) in rabbit and mouse ventricular myocytes, respectively (in whole-cell patch clamp). Both acute and chronic CaMKIIδ_C overexpression shifted voltage dependence of Na^+ channel availability by –6 mV ($P < 0.05$), and the shift was Ca^{2+} dependent. CaMKII also enhanced intermediate inactivation and slowed recovery from inactivation (prevented by CaMKII inhibitors autocamtide 2–related inhibitory peptide [AIP] or KN93). CaMKIIδ_C markedly increased persistent (late) inward I_{Na} and intracellular Na^+ concentration (as measured by the Na^+ indicator sodium-binding benzofuran isophthalate [SBFI]), which was prevented by CaMKII inhibition in the case of acute CaMKIIδ_C overexpression. CaMKII coimmunoprecipitates with and phosphorylates Na^+ channels. In vivo, transgenic CaMKIIδ_C overexpression prolonged QRS duration and repolarization (QT intervals), decreased effective refractory periods, and increased the propensity to develop VT. We conclude that CaMKII associates with and phosphorylates cardiac Na^+ channels. This alters I_{Na} gating to reduce availability at high heart rate, while enhancing late I_{Na} (which could prolong action potential duration). In mice, enhanced CaMKIIδ_C activity predisposed to VT. Thus, CaMKII-dependent regulation of Na^+ channel function may contribute to arrhythmogenesis in HF.

Introduction

Altered Na^+ channel gating was shown to underlie long QT syndrome 3 (LQT3) (1), Brugada syndrome (2), and isolated cardiac conduction defects predisposing to life-threatening ventricular tachyarrhythmias (VTs). However, these mutations are relatively rare. Heart failure (HF) is associated with an increased risk of sudden death mainly caused by VT and fibrillation (3). The mechanisms are poorly understood, but altered Na^+ channel gating may be involved.

Abnormal conduction is the proximate cause of sudden death in HF, and Na^+ channels critically determine conduction velocity (4). A persistent (late) Na^+ current (I_{Na}) was shown to cause prolongation of action potentials (APs) in HF myocytes (5). A tetrodotoxin-sensitive (TTX-sensitive) pathway was implicated in increased intracellular Na^+ concentration ($[Na]_i$) in HF (6).

It is known that calmodulin (CaM) regulates Na^+ channel gating through binding to an IQ-like motif at the C terminus (7). Downstream signaling through Ca^{2+}/CaM-dependent protein kinase II (CaMKII) may be of relevance, but little is known about CaMKII-dependent effects on I_{Na}. CaMKIIδ is the predominant isoform in the heart (8). Upon phosphorylation, CaMKII is known to alter L-type Ca^{2+} channel function, providing an integrative feedback for oscillatory intracellular free Ca^{2+} ($[Ca^{2+}]_i$) (8). In human HF and in an animal HF model, expression and activity of CaMKII are enhanced 2- to 3-fold (9–11). We have shown that transgenic overexpression of cytosolic CaMKIIδ_C induces HF (12, 13). Inhibition of CaMKII was shown to prevent remodeling after myocardial infarction and excessive β-adrenergic stimulation (14). CaMKII has also been linked to VT in a mouse model of hypertrophy (15).

Here we explore the role of CaMKIIδ_C on Na^+ channel function using 2 models. We assessed Na^+ channel function and expression in CaMKIIδ_C-Tg mice, which develop HF. We investigated acute CaMKIIδ_C overexpression (rabbit myocytes) to avoid unspecific adaptations occurring in HF. We show that CaMKIIδ_C regulates Na^+ channel gating and $[Na]_i$, which may have implications for HF.

Results

Steady-state inactivation and activation. To assess whether CaMKIIδ_C regulates Na^+ channels, we measured steady-state inactivation of I_{Na}. Figure 1 shows steady-state inactivation as a function of membrane potential (E_m) in rabbit myocytes. CaMKIIδ_C overexpression in myocytes (hereafter referred to as "CaMKIIδ_C myocytes") but not β-gal overexpression in myocytes (hereafter referred to as "β-gal myocytes") caused a negative voltage shift in I_{Na} steady-state inactivation ($V_{1/2}$: –83.5 ± 0.8 versus –89.7 ± 0.7 mV; $P < 0.05$; Table 1). This reduced the fraction of available Na^+ channels at a given E_m. The slope factor k_∞ was unaltered. This effect was Ca^{2+} dependent.

Nonstandard abbreviations used: AIP, autocamtide 2–related inhibitory peptide: AP, action potential; $[Ca^{2+}]_i$, intracellular free Ca^{2+}; CaM, calmodulin; CaMKII, Ca^{2+}/CaM-dependent protein kinase II; C_m, membrane capacitance; DAD, delayed afterdepolarization; EAD, early afterdepolarization; E_m, membrane potential; HF, heart failure; I_{fast}, fast inactivation; I_{IM}, intermediate inactivation; I_{Na}, Na current; LQT3, long QT syndrome 3; MAP, monophasic AP; $[Na]_i$, intracellular Na concentration; $[Na]_o$, extracellular Na^+ concentration; SR, sarcoplasmic reticulum; TTX, tetrodotoxin; VT, ventricular tachyarrhythmia.

Conflict of interest: The authors have declared that no conflict of interest exists.

Citation for this article: *J. Clin. Invest.* **116**:3127–3138 (2006). doi:10.1172/JCI26620.

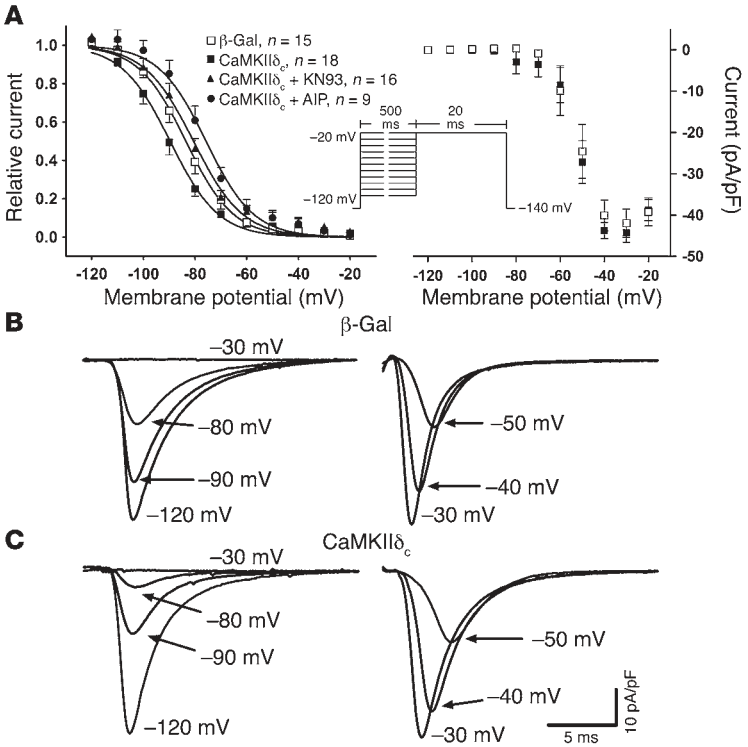

Figure 1
CaMKIIδc enhances steady-state inactivation of rabbit myocyte I_{Na} (10 mM $[Na^+]_o$). (**A**) Mean I_{Na} availability (left) and I_{Na} during conditioning pulses (right; fit parameters in Table 1). In CaMKIIδc myocytes, availability was left-shifted versus β-gal ($P < 0.05$), and this was reversed by CaMKII inhibitors KN93 or AIP ($P < 0.05$). (**B** and **C**) Original I_{Na} traces during prepulses (right) and test pulse (left). I_{Na} amplitudes during prepulses were unaltered by CaMKIIδc (see Figure 2).

When $[Ca^{2+}]_i$ was increased to 500 nM, $V_{1/2}$ was further shifted toward more negative potential ($P < 0.05$; Table 1). All effects were reversed using KN93 or autocamtide 2–related inhibitory peptide (AIP) (Figure 1 and Table 1). Interestingly, both inhibitors increased the fraction of available Na^+ channels and reversed the effects of elevated $[Ca^{2+}]_i$, even in β-gal myocytes, suggesting that there may be some basal CaMKII-dependent Na^+ channel regulation. Similar results were observed using physiologic extracellular Na^+ concentration ($[Na]_o$) and when investigating CaMKIIδC-Tg mice (Table 2). Again, CaMKII inhibition blocked all CaMKIIδC-dependent effects on the E_m dependence of Na^+ channel steady-state inactivation.

Since steady-state inactivation of Na^+ channels depends on both channel activation and inactivation, the current-voltage (I-V) relation of I_{Na} in CaMKIIδC-overexpressing myocytes was assessed

Table 1
Fit parameters of the analysis of I_{Na} inactivation (rabbit, 10 mM $[Na]_o$)

		$[Ca^{2+}]_i$, 100 nM			$[Ca^{2+}]_i$, 500 nM	
		CaMKIIδC (*n*) (β-gal [*n*])	**CaMKIIδC + KN93 (*n*) (β-gal + KN93 [*n*])**	**CaMKIIδC+AIP (*n*) (β-gal +AIP [*n*])**	**CaMKIIδC (*n*) (β-gal [*n*])**	**CaMKIIδC+KN93 (*n*) (β-gal + KN93 [*n*])**
Steady-state inactivation	$V_{1/2}$ (mV)	−89.7 ± 0.7 (18)	−80.6 ± 0.8 (16)[A]	−75.7 ± 1.1 (9)[A]	−95.8 ± 0.6 [16][A]	−85.2 ± 0.9 [9][C]
		(−83.5 ± 0.8 [15])[A]	(−80.8 ± 1.3 [7])[B]	(−77.4 ± 0.9 [8])[B]	(−90.6 ± 1.1 [13])[B]	(−84.6 ± 1.8 [3])[D]
	k_∞ (mV)	9.4 ± 0.6	9.5 ± 0.7	9.2 ± 0.9	9.2 ± 0.5	9.2 ± 0.8
		(9.2 ± 0.7)	(9.2 ± 1.2)	(11.7 ± 0.8)	(10.8 ± 1.0)	(9.2 ± 1.6)
Development of I_{IM}	A	0.4 ± 0.01 (16)	0.32 ± 0.02 (12)[A]	0.32 ± 0.01 (7)[A]	0.44 ± 0.02 (12)[A]	0.3 ± 0.02 (9)[C]
		(0.28 ± 0.02 [13])[A]	(0.21 ± 0.01 [7])[B]	(0.23 ± 0.01 [7])[B]	(0.31 ± 0.03 [10])[B]	(0.34 ± 0.02 [3])
	k_{IM} (s^{-1})	1.1 ± 0.1	0.9 ± 0.2	0.9 ± 0.1	0.9 ± 0.1	0.9 ± 0.2
		(1.2 ± 0.2)	(0.9 ± 0.1)	(1.7 ± 0.1)	(0.9 ± 0.2)	(0.9 ± 0.2)
	y_0	0.48 ± 0.02	0.62 ± 0.02[A]	0.65 ± 0.01[A]	0.34 ± 0.02[A]	0.6 ± 0.02[C]
		(0.66 ± 0.02)[A]	(0.74 ± 0.01)[B]	(0.7 ± 0.01)[B]	(0.54 ± 0.03)[B]	(0.52 ± 0.02)
Recovery from inactivation	A	0.87 ± 0.02 (13)	0.92 ± 0.02 (13)	0.89 ± 0.04 (6)	0.87 ± 0.04 (12)	0.92 ± 0.02 (6)
		(0.86 ± 0.03 [10])	(0.92 ± 0.02 [7])	(0.9 ± 0.03 [6])	(0.86 ± 0.02 [9])	(0.93 ± 0.02 [4])
	τ_{rec} (ms)	18 ± 1.1	12 ± 0.8[A]	7.7 ± 1.2[A]	29.1 ± 4[A]	12.5 ± 0.8[C]
		(12.3 ± 1.2)[A]	(10 ± 0.7)[B]	(10.9 ± 1.2)	(15.7 ± 1.4)[B]	(18 ± 1.2)

Fit parameters (rabbit myocytes, 10 mM $[Na]_o$) for steady-state inactivation (average maximum I_{Na} –5.1 ± 0.2 nA, –41.4 ± 1.6 pA/pF, C_m 127.2 ± 4.3 pF), development of I_{IM} (average maximum I_{Na} –5.3 ± 0.3 nA, –43.8 ± 2 pA/pF, C_m 125.9 ± 4.6 pF), and recovery from inactivation (average maximum I_{Na} –5.2 ± 0.3 nA, –43.7 ± 2.1 pA/pF, C_m 123.5 ± 4.8 pF). Steady-state inactivation was fitted to a standard Boltzmann equation: $h_\infty = 1/\{1 + \exp[(V_{1/2} - V)]/k_\infty\}$. The development of I_{IM} and the recovery from inactivation were fitted with single exponential functions: $y(t) = A \exp(-k_{IM} t) + y_0$ and $y(t) = A[1 - \exp(-t/\tau_{rec})]$, respectively. [A]$P < 0.05$ versus CaMKIIδC 100 nM $[Ca^{2+}]_i$. [B]$P < 0.05$ versus β-gal 100 nM $[Ca^{2+}]_i$. [C]$P < 0.05$ versus CaMKIIδC 500 nM $[Ca^{2+}]_i$. [D]$P < 0.05$ versus β-gal 500 nM $[Ca^{2+}]_i$.

Table 2
Fit parameters of the analysis of I_{Na} inactivation (rabbit and mouse, physiological $[Na]_o$)

		Rabbit		Mouse	
		CaMKIIδc (*n*) (β-gal [*n*])	CaMKIIδc + KN93 (*n*) (β-gal + KN93 [*n*])	Tg CaMKIIδc (*n*) (WT [*n*])	Tg CaMKIIδc + KN93 (*n*) (WT + KN93 [*n*])
Steady-state inactivation	$V_{1/2}$ (mV)	–75.7 ± 0.8 (15) (–71.3 ± 0.9 [10])[A]	–70.9 ± 0.7 (21)[A] (–71.7 ± 0.7 [17])	–71.5 ± 0.9 (7) (–66.6 ± 0.7 [5])[A]	–65 ± 1.3 (3)[A]
	k_∞ (mV)	7.2 ± 0.7 (7.5 ± 0.8)	8.2 ± 0.6 (7.2 ± 0.6)	8.4 ± 0.7 (7.7 ± 0.6)	7.7 ± 1.1
Development of I_{IM}	A	0.27 ± 0.03 (16) (0.18 ± 0.02 [10])[A]	0.22 ± 0.02 (20)[A] (0.13 ± 0.02 [19])[B]	0.28 ± 0.04 (11) (0.06 ± 0.02 [17])[A]	0.13 ± 0.02 (4)[A] (0.02 ± 0.01 [10])[B]
	k_{IM} (s^{-1})	0.8 ± 0.2 (0.8 ± 0.2)	0.7 ± 0.1 (0.7 ± 0.2)	0.6 ± 0.2 (0.6 ± 0.3)	0.6 ± 0.2 (0.6 ± 0.4)
	y_0	0.69 ± 0.03 (0.8 ± 0.02)[A]	0.76 ± 0.02[A] (0.84 ± 0.01)[B]	0.71 ± 0.04 (0.94 ± 0.02)[A]	0.87 ± 0.02[A] (0.98 ± 0.01)[B]
Recovery from inactivation	A	0.93 ± 0.02 (15) (0.95 ± 0.02 [12])	0.96 ± 0.01 (21) (0.95 ± 0.01 [20])	0.96 ± 0.03 (8) (0.99 ± 0.02 [17])	1 ± 0.03 (3) (0.99 ± 0.02 [4])
	τ_{rec} (ms)	9 ± 0.7 (6 ± 0.4)[A]	7.9 ± 0.4[A] (6.5 ± 0.3)	8.2 ± 0.8 (6 ± 0.4)[A]	4.9 ± 0.6[A] (2.7 ± 0.3)[B]

Fit parameters (140 mM $[Na]_o$, 100 nM $[Ca^{2+}]_i$) for analysis as shown in Table 1 (Boltzmann equation for steady-state inactivation and single exponential fits for development of I_{IM} and recovery from inactivation). Steady-state inactivation, average maximum I_{Na} –8.9 ± 0.4 nA, –70.3 ± 3 pA/pF, C_m 129.7 ± 4.4 pF for rabbit and –17.1 ± 2.2 nA, –78.6 ± 8.5 pA/pF, C_m 218.1 ± 12.8 pF for mouse. Development of I_{IM}, average maximum I_{Na} –9.4 ± 0.4 nA, –73.9 ± 3.3 pA/pF, C_m 130.8 ± 4.4 for rabbit and –11.7 ± 0.8 nA, –46.3 ± 3.4 pA/pF, C_m 269.1 ± 16.1 pF for mouse. Recovery from inactivation, average maximum I_{Na} –9.4 ± 0.4 nA, –72.9 ± 3.1 pA/pF, C_m 134.8 ± 4.8 pF for rabbit and –15.3 ± 1.4 nA, –58.9 ± 5.3 pA/pF, C_m 271 ± 12.7 pF for mouse. [A]$P < 0.05$ versus CaMKIIδ_C (rabbit) and CaMKIIδ_C-Tg (mouse). [B]$P < 0.05$ versus β-gal and WT.

(basic cycle length, 2 seconds; Figure 2), with no difference in maximal current density observed. There was also no alteration in the E_m dependence of Na^+ channel conductance (G), suggesting that Na^+ channel activation is not altered by CaMKII. Therefore, the differences in steady-state inactivation are most likely ascribable to altered inactivation.

Intermediate inactivation and recovery from inactivation. We additionally investigated intermediate inactivation (I_{IM}), a form of Na^+ channel inactivation that accumulates over a few hundred milliseconds (after fast inactivation [I_{fast}]) and recovers much more slowly at negative E_m than I_{fast}. Enhanced I_{IM} has been implicated in Brugada syndrome (2) and has been suggested to be a consequence of CaM-dependent Na^+ channel regulation (7). I_{IM} was measured using depolarizations of variable duration (P_1) followed by a 20-ms recovery period at –140 mV, allowing for recovery from fast inactivation but not from I_{IM}. The following test pulse (P_2) to –20 mV activated all channels not in I_{IM} (Figure 3A). Physiologically, only a small fraction of Na^+ channels undergo I_{IM} and reduce the amount of channels available for the second excitation. Figure 3 shows that CaMKIIδ_C overexpression significantly increased the fraction of channels undergoing I_{IM}. Curve fitting analysis revealed that the amplitude *A* was significantly increased, whereas the rate constant k_{IM} was unaltered (Table 1). Thus, CaMKIIδ_C may increase the fraction of channels that can enter I_{IM}, but not the rate constant of development of I_{IM}. Again, this effect was Ca^{2+} dependent. At high $[Ca^{2+}]_i$ (500 nM), the amplitude of I_{IM} was significantly increased (Table 1). All effects were reversible with KN93 or AIP, which were also effective in β-gal myocytes.

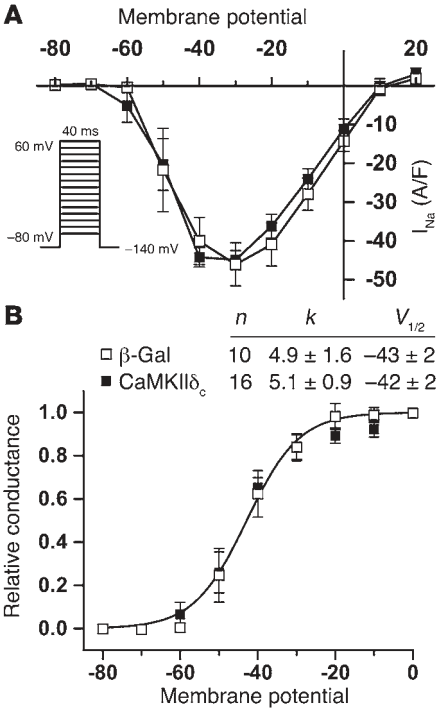

Figure 2
E_m dependence of I_{Na} activation in rabbit myocytes (10 mM $[Na^+]_o$). (**A**) Current-voltage relation (I-V) for CaMKIIδ_c versus β-gal myocytes. (**B**) I_{Na} activation curve, with relative conductance derived from maximal chord conductance and reversal potential (E_{rev}) for each I-V, and peak $I_{Na}/(E_m - E_{rev})$. The resulting conductance was normalized to the maximal chord conductance (usually between –10 and 0 mV). CaMKIIδ_C had no effect on voltage for half-activation $V_{1/2}$ or slope factor *k* (mV). Maximal I_{Na} was –4.3 ± 0.2 nA and –49.8 ± 2.4 pA/pF (C_m, 88.2 ± 5.7 pF) for CaMKIIδ_c versus –4.1 ± 0.5 nA and –42.8 ± 4.4 pA/pF (C_m, 103.8 ± 17.7 pF) for β-gal (*P* = NS).

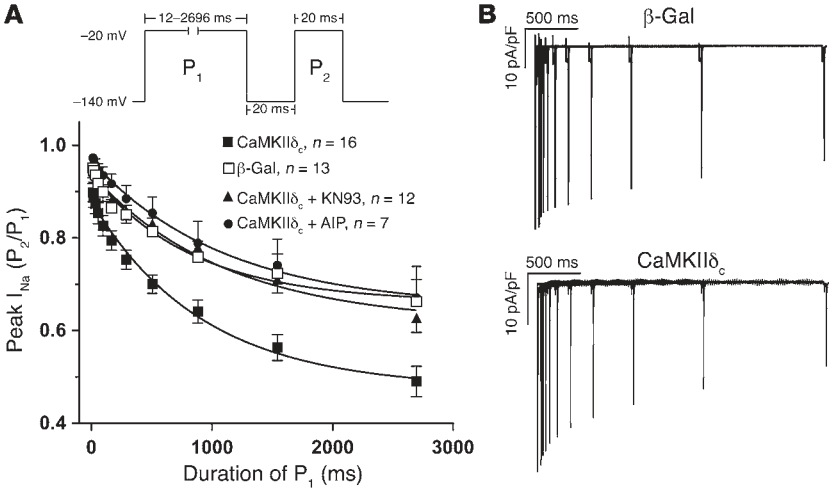

Figure 3
$CaMKII\delta_c$ increases I_{IM} of I_{Na} in rabbit myocytes (10 mM $[Na^+]_o$). (**A**) Increasing conditioning pulse duration (P_1) reduced peak I_{Na} assessed with a second pulse (P_2). $CaMKII\delta_c$ increased the amount of accumulating I_{IM} (versus β-gal; $P < 0.05$), an effect reversed by KN93 or AIP ($P < 0.05$). Mean data were fitted to a single exponential (see Table 1). (**B**) Original traces of peak I_{Na} (at P_2) for different P_1 durations.

As for steady-state inactivation, a similarly enhanced I_{IM} was observed using a more physiologic $[Na]_o$ and in $CaMKII\delta_C$ transgenics (Table 2). Again, CaMKII inhibition blocked $CaMKII\delta_C$-dependent effects. In WT and β-gal myocytes, KN93 reduced the amount of I_{IM} even further (Table 2). Thus, CaMKII may contribute to I_{IM}, and there may be some basal CaMKII-dependent I_{IM} in WT mouse and control rabbit cells (with lower basal I_{IM} in WT).

Inactivation and recovery from inactivation are closely related and critically determine channel function. Recovery from inactivation was investigated using a sustained depolarization at a time scale that initiates fast and I_{IM} (1,000 ms), followed by recovery intervals of increasing durations and a subsequent test pulse (Figure 4A). In comparison to that of control, recovery from inactivation was slowed in $CaMKII\delta_C$ myocytes (Figure 4). Data were fit to a single exponential relation. The time constant for recovery from inactivation (τ_{rec}) increased from 12.3 ± 1.2 ms (β-gal) to 18 ± 1.1 ms ($CaMKII\delta_C$; Table 1), indicating that recovery was slower by nearly 50% in $CaMKII\delta_C$ myocytes. Either KN93 or AIP returned τ_{rec} to control levels (Table 1). KN93 by itself slightly reduced τ_{rec} in β-gal myocytes, consistent with a basal CaMKII-dependent effect on I_{Na} recovery from inactivation. The effect of $CaMKII\delta_C$ on τ_{rec} was Ca^{2+} dependent, because at high $[Ca^{2+}]_i$ (500 nM), τ_{rec} increased further, and KN93 completely reversed this (Figure 4A and Table 1).

These results indicate that $CaMKII\delta_C$ activity substantially slows I_{Na} recovery from inactivation. This may reflect, in part, slower recovery from I_{IM}, as there was more I_{IM} in the cases where recovery was prolonged. The slower I_{Na} recovery could also limit I_{Na} availability, especially at high heart rates.

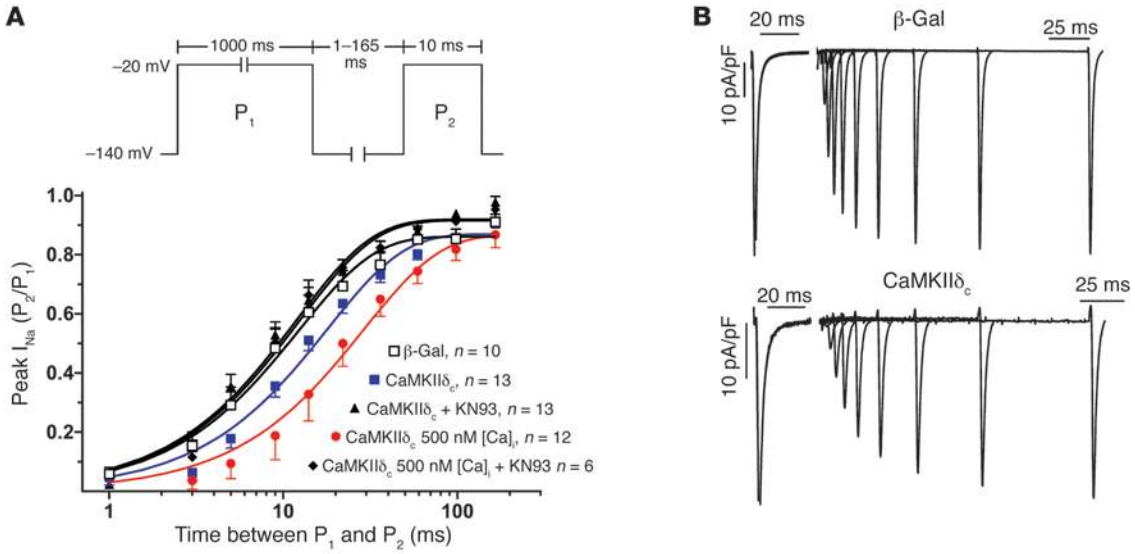

Figure 4
$CaMKII\delta_c$ slows I_{Na} recovery from inactivation in rabbit myocytes (10 mM $[Na^+]_o$). (**A**) Increasing durations of recovery interval between conditioning pulse (P_1, causing I_{Na} and inactivation) and test pulse (P_2). $CaMKII\delta_C$ significantly slowed recovery versus β-gal, an effect blocked upon CaMKII inhibition (KN93; $P < 0.05$). Elevation of $[Ca^{2+}]_i$ to 500 nM in myocytes overexpressing $CaMKII\delta_C$ further slowed recovery, and KN93 completely inhibited this effect. Mean data were fit to a single exponential (fit parameters in Table 1). (**B**) Original traces of I_{Na} for different recovery intervals.

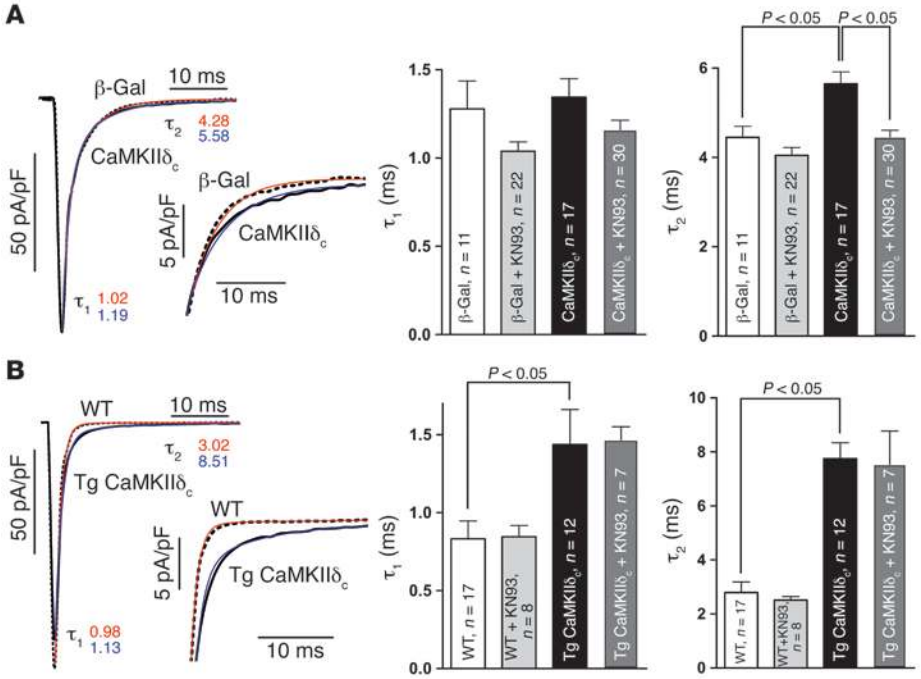

Figure 5
CaMKIIδc slows fast decay of I_{Na}. (**A**) Original traces show that CaMKIIδc slows fast I_{Na} inactivation in rabbit myocytes versus β-gal. I_{Na} decay (first 50 ms) was fit with a double exponential: $y(t) = A_1 \exp(-t/\tau_1) + A_2 \exp(-t/\tau_2) + y_0$. Fits and τ_1 and τ_2 (ms) are shown in red (β-gal) and blue (CaMKIIδc). Deceleration of I_{Na} decay was significant in τ_2 but not in τ_1. KN93 could reverse the slowing of τ_2 by CaMKIIδC. (**B**) In CaMKIIδC-Tg mice, both τ_1 and τ_2 were slowed compared with those in WT mice. Fits to the original traces and τ_1 and τ_2 values (ms) are shown in red (WT) and blue (CaMKIIδC-Tg). KN93 did not reverse these effects. Average peak I_{Na} was –10.2 ± 0.3 nA, –79.8 ± 2.7 pA/pF, C_m 132.7 ± 4 pF for rabbit and –14.2 ± 0.6 nA, –58.9 ± 2.9 pA/pF, C_m 255.3 ± 11 pF for mouse.

The CaMKIIδC-dependent slowing of Na^+ channel recovery was also seen in physiologic $[Na^+]_o$, and the effect could be measured in CaMKII transgenics (Table 2). Consistently, the effect of CaMKIIδC overexpression was completely reversible with CaMKII inhibition.

Fast, open-state inactivation and $[Na]_i$. When Na^+ channels open, they close very rapidly, within 10–20 ms, a process called fast or open-state inactivation. In contrast to I_{IM}, for which no structural correlate has been found yet, the cytoplasmic linker between domains III and IV and the C terminus of the Na^+ channel protein has been suggested to underlie I_{fast}. Mutations in these regions are known to disrupt this process, leading to LQT3. Since the putative target of CaMKII-dependent regulation could be located there, we investigated the effect of CaMKIIδC on fast I_{Na} decay. Acute CaMKIIδC overexpression significantly slowed the late component of fast I_{Na} inactivation (see τ_2, Figure 5A), which was sensitive to KN93.

When myocytes from CaMKIIδC-Tg mice were assessed, initial and late components (τ_1, τ_2; Figure 5B) of I_{Na} decay were significantly slowed compared with those of WT myocytes. However, KN93 did not reverse the effect in mice, leaving more open the role of CaMKII in this transgenic mouse model.

Incomplete I_{Na} inactivation during the AP can influence AP duration and $[Na]_i$ and can also be arrhythmogenic. Figure 6, A and B, shows a distinct persistent I_{Na} component in both acute and chronic CaMKII overexpression that is not seen in β-gal rabbit or WT mouse myocytes. Again, KN93 prevented this persistent I_{Na} in CaMKIIδC rabbit myocytes, but not in mice.

To assess the impact of these alterations in late I_{Na} on Na^+ influx, we integrated the late I_{Na} (50–500 ms) and normalized it to the cytosolic volume. For rabbit, values were (in μM): CaMKIIδC (versus β-gal), –7.47 ± 0.77 (–3.04 ± 0.92); and CaMKIIδC+KN93 (versus β-gal plus KN93), –3.35 ± 0.36 (–2.84 ± 0.63). For mouse, integrals were Tg (versus WT), –8.23 ± 1.60 (–2.05 ± 0.60); and Tg plus KN93 (versus WT plus KN93), –7.9 ± 2.46 (–1.89 ± 0.61). If the amount of Na^+ entry was extrapolated to 1 minute, the Na^+ influx was 1.0 ± 0.1 versus 0.4 ± 0.1 mM/min (rabbit, CaMKIIδC versus β-gal) and –1.1 ± 0.21 versus –0.27 ± 0.08 mM/min (mouse, Tg versus WT). Interestingly, the increased amount of Na^+ influx upon CaMKII overexpression strikingly resembles the TTX-sensitive Na^+ entry suggested to cause elevated $[Na]_i$ in an HF model with increased CaMKII activity (6, 11).

To assess whether the CaMKII-dependent alterations in I_{Na} gating cause increased $[Na]_i$, we measured $[Na]_i$ in field-stimulated myocytes. In CaMKIIδC-overexpressing rabbit myocytes, $[Na]_i$ was significantly increased at all stimulation frequencies compared with that in control. This increase was completely reversed by KN93 (Figure 6C). In CaMKIIδC-Tg mice, $[Na]_i$ was also significantly elevated (versus WT), but the increase was not reversible with KN93 (Figure 6D).

Association of CaMKII with Na^+ channels and CaMKII-dependent phosphorylation. Coimmunoprecipitation studies revealed that CaMKII associates with Na^+ channels in both mouse and rabbit tissue (anti-Pan Na_v, an antibody recognizing all Na^+ channel isoforms; Figure 7, A and B). Western blotting of the immunoprecipitates repeated with cardiac-specific anti-$Na_v1.5$ showed similar results (data not shown), proving that the cardiac Na^+ channel isoform interacts with CaMKII. Using immunocytological staining, CaMKIIδC and Na^+ channels were found to be colocalized in CaMKIIδC-overexpressing myocytes (Figure 7C). No colocalization was seen when the anti-HA antibody was used in control-transfected myocytes (data not shown).

CaMKII-dependent phosphorylation of Na^+ channels was investigated using ATP-γ-^{32}P. First, we exposed immunoprecipitated Na^+ channels from WT mice to purified preactivated exogenous CaMKII (Figure 7D). Exogenous CaMKII clearly phosphorylated Na^+ channels, and this effect was inhibited when KN93 or AIP were included, but not when PKA and PKC were blocked (Figure 7E).

Since endogenous CaMKII associates with the Na^+ channel, we tested whether endogenous myocyte CaMKII can phosphorylate Na^+ channels in the myocyte (Figure 7F). Saponin-permeabilized rabbit myocytes were exposed for 5 minutes to internal solution at 50 nM

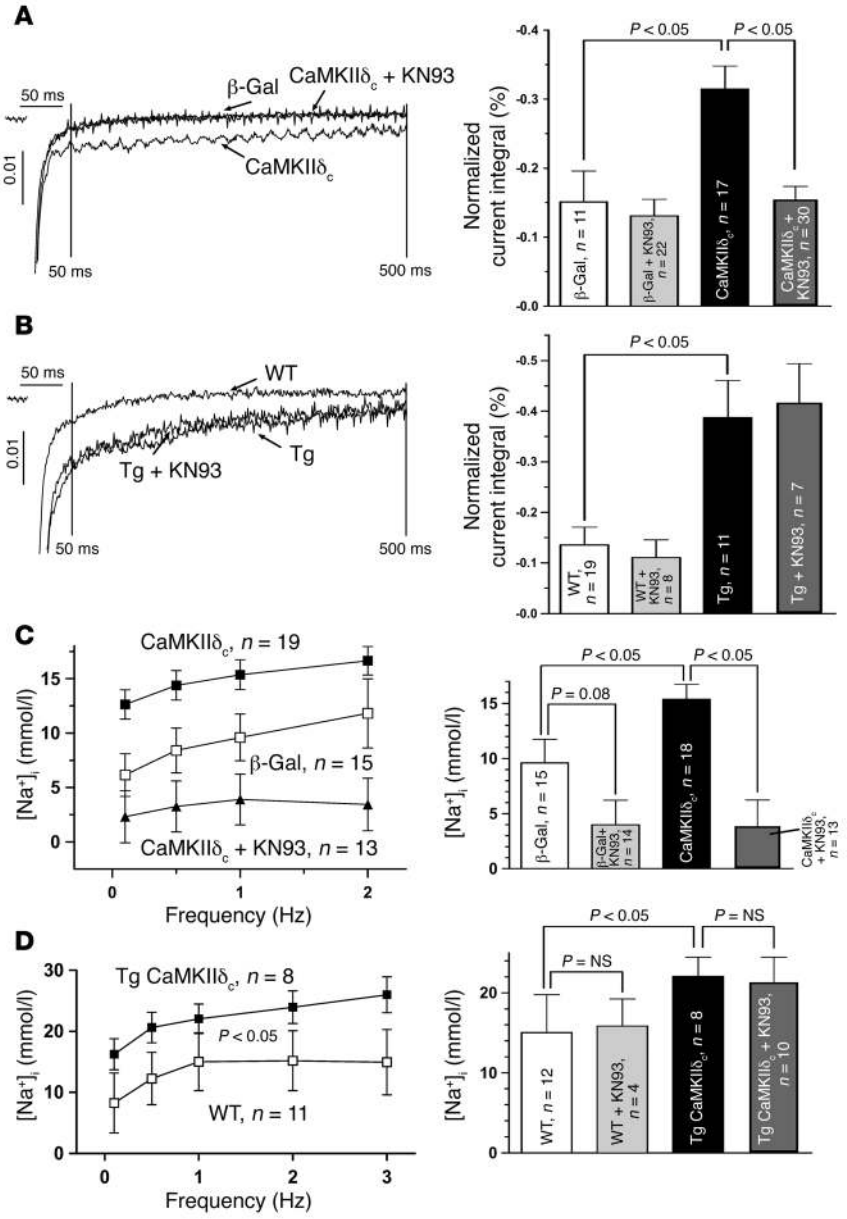

Figure 6
CaMKIIδc enhances late I_{Na} and increases $[Na]_i$. I_{Na} elicited at –20 mV (for 1,000 ms) was leak subtracted and normalized to peak I_{Na}. Current was integrated between 50 and 500 ms and normalized to the I_{Na} integral if no inactivation had occurred. (**A**) Original traces and mean data of normalized late I_{Na}. CaMKIIδC overexpression significantly increased late I_{Na} (reversed with KN93). (**B**) CaMKIIδC-Tg mice also showed late I_{Na}, but this was not reversible with KN93. Average peak I_{Na} was –10.2 ± 0.3 nA, –79.8 ± 2.7 pA/pF, C_m 132.7 ± 4 pF for rabbit and –14.3 ± 0.6 nA, –58.1 ± 2.8 pA/pF, C_m 259.7 ± 11.6 pF for mouse. (**C**) Mean $[Na]_i$ at different stimulation frequencies (left) and at 1 Hz (right) in rabbit myocytes. $[Na]_i$ was elevated in CaMKIIδc myocytes at all frequencies ($P < 0.05$) and reduced by KN93 ($P < 0.05$). (**D**) Mean data for CaMKIIδC-Tg mice also showing elevated $[Na]_i$ (versus WT; $P < 0.05$), but this was not reversed by KN93.

$[Ca^{2+}]$ or 500 nM $[Ca^{2+}]$ plus 2 μM CaM (to activate endogenous CaMKII). The extent of CaMKII-dependent Na^+ channel phosphorylation was assessed afterward by Na^+ channel immunoprecipitation and subsequent back-phosphorylation with exogenous preactivated CaMKII and ATP-γ-^{32}P. Activation of endogenous CaMKII (500 nM $[Ca^{2+}]$) reduced back-phosphorylation (lane 2 versus lane 1), indicating increased Na^+ channel phosphorylation upon activation of cellular CaMKII. Inclusion of AIP in the myocyte preincubation prevented the increased phosphorylation (lane 3, Figure 7F). Interestingly, overexpression of CaMKIIδC increased the phosphorylation level (decreased back-phosphorylation) of Na^+ channels at 50 nM $[Ca^{2+}]$ to a level comparable to that attained in the control at the 500 nM $[Ca^{2+}]$ incubation. Thus, CaMKII associates with the Na^+ channel, and the endogenous CaMKII can phosphorylate the channel.

Western blotting revealed significantly increased Na^+ channel expression in hearts from Tg mice (1.6-fold versus WT; Figure 7G). However, I_{Na} was not significantly different in Tg versus WT hearts (–127.1 ± 16 pA/pF versus –109 ± 22.4 pA/pF, respectively, at –30 mV; $n = 5$ versus 9; P = NS; average maximum I_{Na}, –15.1 ± 1 nA, –115.5 ± 15.2 pA/pF, membrane capacitance [C_m], 197.3 ± 21.7 pF). In contrast, Na^+ channel expression was not altered in rabbit myocytes acutely overexpressing CaMKIIδC (Figure 7H).

CaMKII and arrhythmias. To test whether CaMKIIδC mice were prone to VT, we performed electrophysiological measurements in vivo (Figure 8). Application of 2 consecutive premature beats via programmed electrical stimulation induced monomorphic and polymorphic VT. In addition, 1 Tg mouse died because of spontaneous ventricular fibrillation immediately after recordings were started. In contrast, no arrhythmias were observed in WT mice (Figure 8, A and C). In separate experiments, application of isoproterenol (2 mg/kg, i.p.) increased heart rate from 460 ± 50 to 680 ± 10 bpm for WT mice, but no arrhythmias were observed (Figure 8, B and C). In contrast, in Tg mice, isoproterenol infusion induced monomorphic VT. Analysis of resting ECG parameters

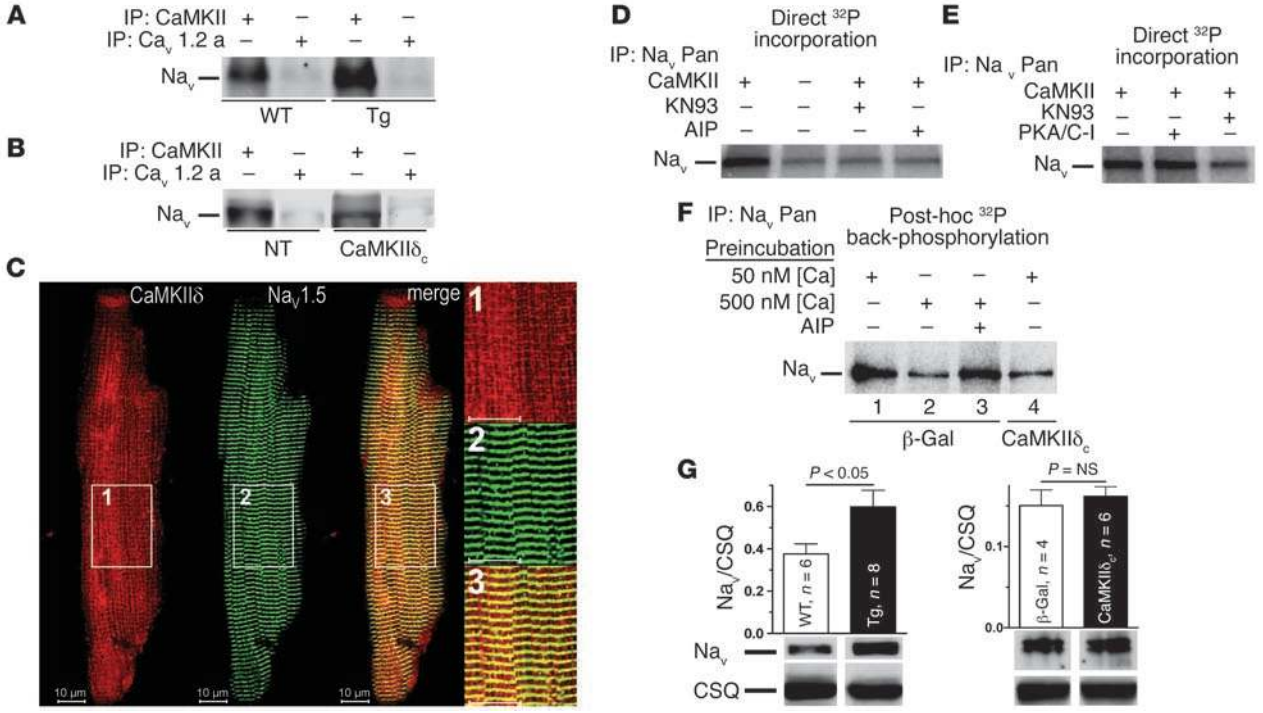

Figure 7

CaMKII-dependent association with and phosphorylation of Na^+ channels. (**A** and **B**) Equal amounts of CaMKII were IP from mouse hearts (**A**, Tg versus WT) and rabbit myocytes (**B**, CaMKIIδ_c versus nontransfected cells) and subjected to immunoblotting. CaMKII IP showed CaMKII association with Na^+ channels in WT and Tg hearts ($n = 3$ and $n = 3$, respectively), while IP with polyclonal rabbit anti-$Ca_v1.2a$ did not. Similar results were seen in rabbit myocytes (CaMKIIδ_C and nontransfected cells, $n = 4$ and $n = 2$, respectively). (**C**) Colocalization of CaMKII and Na^+ channel in rabbit myocytes with immunocytological staining. (**D** and **E**) Autoradiograms measuring ^{32}P incorporation into Na^+ channels. Equal amounts of Na^+ channels were immunoprecipitated from WT mouse hearts ($n = 3$) and directly phosphorylated with or without CaMKII, KN93 (50 μM), AIP (5 μM), or PKA/PKC inhibitor cocktail (PKA/C-I; 1 μM). (**F**) Endogenous CaMKII-dependent Na^+ channel phosphorylation was activated in permeabilized rabbit myocytes by preincubating for 5 minutes in internal solutions of 500 nM [Ca^{2+}] plus 2 μM CaM (versus 50 nM [Ca^{2+}]). Sites not already phosphorylated were subsequently back-phosphorylated in Na^+ channel immunoprecipitates (equal amounts) by exogenous preactivated CaMKII and ATP-γ-^{32}P. The intensity of ^{32}P is inversely related to the CaMKII-dependent phosphorylation during preincubation. (**G** and **H**) Western blots (anti-Na_v Pan) show upregulation of Na^+ channel expression in CaMKIIδ_C-Tg versus WT mice (relative to calsequestrin [CSQ]) but unaltered expression in CaMKIIδ_C rabbit myocytes (data pooled for MOI 10 and 100).

(Figure 8D) revealed that the corrected QT (QT_c) interval and QRS duration were significantly prolonged in Tg versus WT mice. Interestingly, the PR interval was significantly shortened in Tg mice. CaMKII has been previously implicated in AV nodal conduction (16). To assess whether CaMKIIδ_C overexpression alters AP duration depending on the heart rate, monophasic APs (MAPs) were recorded in isolated perfused hearts. After AV node ablation, Tg hearts had higher intrinsic ventricular heart rates. Spontaneous basic cycle lengths (BCLs) were 325 ± 30 ms (WT) versus 231 ± 16 ms (Tg) ($n = 21$ versus 22; $P < 0.05$). At high pacing frequencies (BCL, 100 ms), MAP duration was not significantly different for Tg versus WT hearts (Figure 8, E and F). It is possible that enhanced steady-state Na^+ channel inactivation and disturbed open-state inactivation may counterbalance each other. At lower pacing frequencies physiological for mice, MAP duration was significantly prolonged in Tg hearts. This was not reversible by CaMK inhibition, suggesting that other effects, possibly related to adaptation or HF, also affect repolarization in the chronic CaMKII expression model.

The effective refractory period (ERP) was decreased in Tg hearts (WT, 27 ± 3 ms, Tg: 20 ± 4 ms; $n = 14$ versus 21; $P < 0.05$), resulting in progressive encroachment of excitation, a scenario known to cause VT (17).

Discussion

The present study shows for the first time to our knowledge that CaMKII regulates Na^+ channel function in myocytes, most likely by association with and phosphorylation of Na^+ channels. This is based on our findings that CaMKII coimmunoprecipitates with and phosphorylates Na^+ channels; and that acute CaMKIIδ_C overexpression slows fast I_{Na} inactivation, enhances late I_{Na}, increases $[Na]_i$, but also enhances accumulation of intermediate I_{Na} inactivation, slows recovery from inactivation, and shifts steady-state inactivation of Na^+ channels to more negative E_m in a Ca^{2+}-dependent manner. Moreover, all of these effects could be reversed with CaMKII inhibition. All these effects were also seen in Tg mice overexpressing CaMKIIδ_C, although impaired inactivation and elevated $[Na]_i$ were not reversed by acute CaMKII inhibition. Overall, these effects prolong Na^+ influx during depolarization (possibly explaining enhanced $[Na]_i$) but increase steady-state inactivation of Na^+ channels at shorter diastolic intervals. This could be particularly arrhythmogenic, and since CaMKII is elevated in HF (9, 10), these effects could cause an acquired form of arrhythmogenesis. Indeed, the altered Na^+ channel phenotype caused by CaMKII is very similar to that caused by the *1495InsD* mutation in human $Na_v1.5$ that is linked with features common to LQT3 and Brugada syndrome

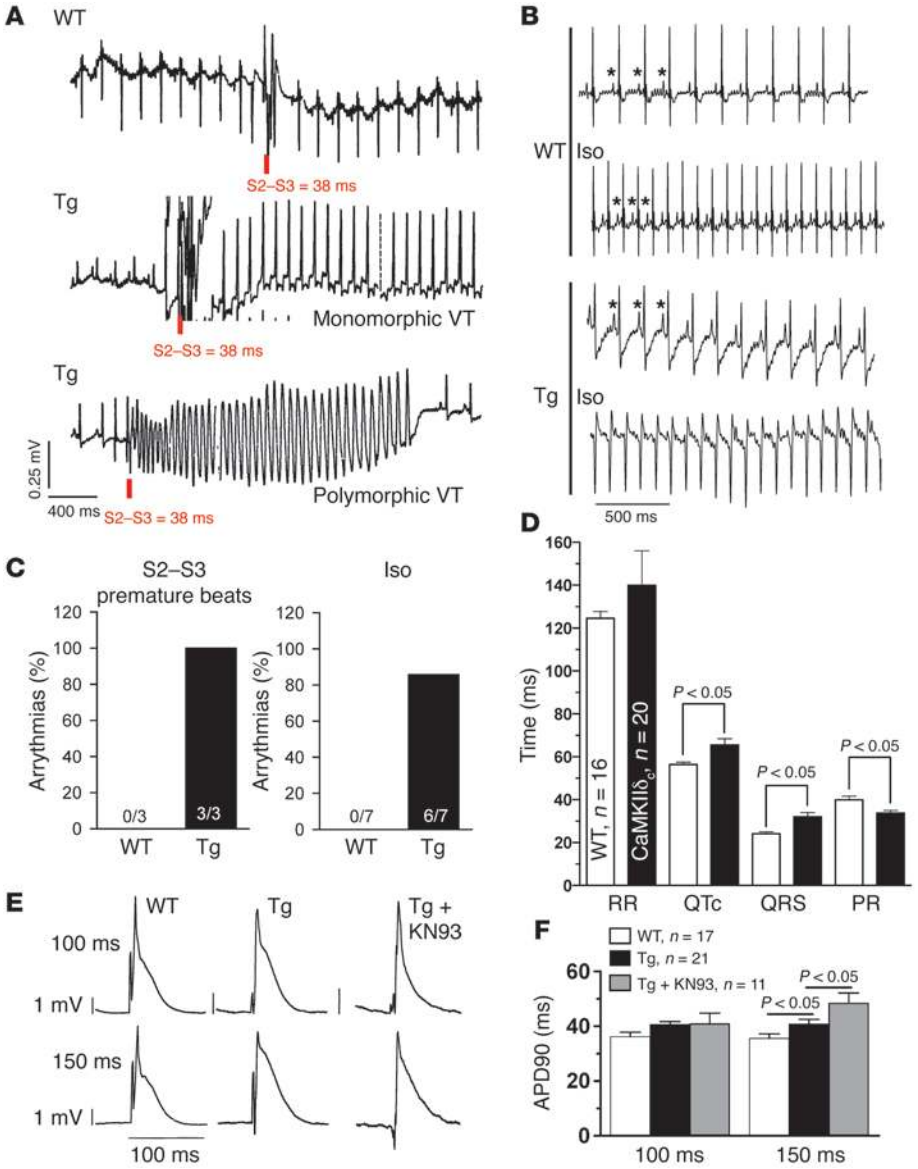

Figure 8
Arrhythmias in CaMKIIδ_C-Tg mice. (**A**) Original ECG traces during programmed electrical stimulation in vivo. In WT mice, 2 consecutive premature beats (S2-S3, coupling interval 38 ms) did not induce arrhythmias (top). In contrast, in 2 different Tg mice, the same protocol induced monomorphic (middle) or polymorphic VT (bottom). (**B**) Representative ECG traces before and after isoproterenol (Iso) administration. P-waves (indicated by asterisks) were apparent during normal rhythms (WT with or without isoproterenol) but were absent in Tg mice after isoproterenol administration. This apparent AV dissociation indicates arrhythmia. (**C**) Frequency of arrhythmia induction was significant in Tg but not WT mice for both programmed electrical stimulation (left) and isoproterenol administration (right). (**D**) Resting ECG parameters (RR interval, corrected QT [QT_c] interval, QRS duration, and PR interval). (**E**) Right-ventricular MAPs from hearts paced at basic cycle lengths (BCLs) of 100 (top) and 150 ms (bottom) for WT mouse hearts (left), Tg mouse hearts (middle), and Tg mouse hearts during infusion with KN93 (right). (**F**) Mean MAP durations at 90% repolarization (APD90). At slower heart rates (BCL, 150 ms), APD90 was significantly prolonged in Tg versus WT mice (but could not be reduced by KN93). At higher heart rates, there was no significant prolongation of APD90 in Tg versus WT.

(18, 19). CaMKIIδ_C-Tg mice were also prone to VT (with reduced effective refractory period, prolonged QRS duration, and disturbed repolarization). While Na^+ channel–independent effects could also contribute to this arrhythmogenesis in CaMKIIδ_C-Tg mice, the documented Na^+ channel phenotype may well be involved.

Na^+ channel regulation by kinases. Na^+ channels are isoform-specifically regulated by kinases including PKA and PKC. PKA-dependent phosphorylation (at Ser526 and Ser529) in the I-II cytoplasmic linker increases whole-cell conductance without altering channel gating resulting from an increased number of functional Na^+ channels, possibly by altering channel trafficking, although cAMP-dependent enhancement of Na^+ channel steady-state inactivation has also been reported (20). PKC-dependent phosphorylation (Ser1505) in the III-IV linker reduces maximal conductance and enhances steady-state inactivation (20).

Deschênes et al. (21), using heterologous Na^+ channel expression, showed that the CaMK inhibitor KN93 slowed I_{Na} decay and shifted steady-state inactivation in the depolarizing direction, but the specific CaMKII inhibitor AIP did not alter I_{Na} gating. They concluded that a CaMK other than CaMKII (e.g., CaMKIV) might have been responsible for I_{Na} modulation. However CaMKIV expression levels in heart are low and primarily nuclear (8), so that CaMKIV is unlikely to modulate I_{Na}. Here we show that overexpression of the predominant cardiac cytosolic CaMKIIδ_C enhanced steady-state and I_{IM} of Na^+ channels. Thus, some effects previously attributed to CaM may actually be mediated by CaMKIIδ_C. In the present study, AIP reversed the effect of CaMKIIδ_C overexpression on steady-state I_{Na} inactivation but also produced smaller shifts in control myocytes (Table 2). This is consistent with some baseline CaMKIIδ_C effect on Na^+ channels in β-gal.

CaMKIIδ_C association and CaMKII-dependent phosphorylation. CaM associates with Na^+ channels (to an IQ motif in the C terminus) (7, 22). We show here that CaMKIIδ_C also associates with Na^+ channels. We also show that exogenous CaMKII can phosphorylate Na^+ channels and, importantly, that endogenous CaMKII in rabbit myocytes can phosphorylate the Na^+ channel at a $[Ca^{2+}]_i$

that is physiologically relevant (500 nM). Moreover, when CaMKII was overexpressed in these myocytes, the Na^+ channel was more phosphorylated even at diastolic $[Ca^{2+}]_i$ level (50 nM). These results suggest that the observed CaMKII- and $[Ca^{2+}]_i$-dependent I_{Na} gating changes (Figures 1–6) may be due to Na^+ channel phosphorylation by CaMKII that is associated with the Na^+ channel.

It is unclear whether CaM preassociated with the Na^+ channel participates in activating CaMKII. However, Na^+ channels may, like many ion channels, be a multiprotein regulatory complex (23).

In the present study, acute CaMKIIδ_C overexpression did not alter functional I_{Na} expression, according to maximal I_{Na} density and protein expression levels. This suggests that CaMKIIδ_C-dependent Na^+ channel regulation may not involve primary effects on Na^+ channel expression or trafficking. However, Tg mice exhibiting HF showed significantly more Na^+ channel expression but unaltered maximal I_{Na} density. This could be a consequence of the HF phenotype, but limited available data suggest that peak I_{Na} density is unaltered in HF (24). Possibly, CaMKII-dependent reduction in I_{Na} availability in rapidly beating Tg mouse hearts causes a compensatory upregulation of Na^+ channel expression. However, the unaltered peak I_{Na} may also mean that some Na^+ channels are less functional (e.g., due to altered channel type, internalization, gating behavior).

Enhanced steady-state and I_{IM}. Several types of I_{Na} inactivation have been distinguished (3): (a) I_{fast} occurring over 2–10 ms (in our analysis with 2 time constants) and recovers rapidly at negative E_m; (b) I_{IM}, which accumulates after I_{fast} has occurred (over hundreds of milliseconds) and recovers more slowly; (c) slow inactivation from the open state (over hundreds of milliseconds); and (d) ultra-slow inactivation, which occurs over many seconds (not studied here). These can all influence Na^+ channel steady-state inactivation, AP duration, and Na^+ flux balance.

CaMKIIδ_C overexpression shifted steady-state inactivation of I_{Na} to more negative E_m and increased the fraction of channels undergoing I_{IM}. Since these recover with slower kinetics, fewer channels would be available for the next excitation at normal heart rates. These effects are thus interrelated functionally (and possibly mechanistically). Indeed, both effects were reversed by CaMKII inhibition. A similar reduction in channel function was shown to underlie Brugada syndrome (2).

Impairment of I_{fast} and $[Na]_i$. Acute CaMKIIδ_C overexpression also slowed fast I_{Na} inactivation (Figure 5A), enhanced late I_{Na} (Figure 6A), and increased $[Na]_i$ (Figure 6C). All effects were prevented by CaMKII inhibition, implicating acute effects of CaMKII. These 3 effects are also functionally related and perhaps mechanistically associated. Slowed I_{Na} inactivation could prolong AP duration, leading to early afterdepolarizations (EADs) or LQT3-like propensity for arrhythmias. In addition, the elevated $[Na]_i$ as a consequence of slowed I_{Na} inactivation would tend to cause Ca^{2+} overload–induced spontaneous sarcoplasmic reticulum (SR) Ca^{2+} release and transient inward current (via Na^+/Ca^{2+} exchange) that underlie delayed afterdepolarizations (DADs) (3).

In HF, these arrhythmogenic effects could be exacerbated by the already elevated $[Na]_i$ (attributed to TTX-sensitive Na^+ entry) and elevated Na^+ entry via slowly inactivating or noninactivating I_{Na} (5, 6, 25). The increased CaMKII expression and activation in HF (9–11) could produce the gamut of I_{Na} and $[Na]_i$ alterations described here upon CaMKIIδ_C overexpression (enhancing arrhythmogenesis in HF). The elevated $[Na]_i$ reported here is unlikely to be explained by a Na^+ "window current" (occurring at E_m where steady-state activation and inactivation curves overlap) (26). This is because the activation curve is unaltered, while steady-state inactivation is shifted in the hyperpolarizing direction, a combination which would reduce window I_{Na}.

Acute and chronic CaMKIIδ_C overexpression produced the same qualitative changes in I_{Na} gating and $[Na]_i$, and for acute overexpression, all of the effects could be completely reversed by CaMKII inhibition. However, in CaMKIIδ_C-Tg mice, some of these changes (slowed open state I_{Na} inactivation, persistent I_{Na}, elevated $[Na]_i$) were not reversed by KN93 application. Thus while CaMKIIδ_C can mediate the whole array of I_{Na} and $[Na]_i$ effects (based on the acute adenoviral studies with and without KN93 or AIP), there may be other effects in chronic HF or CaMKIIδ_C overexpression that mimic or sustain the CaMKII effect on slowing I_{Na} inactivation. It is not clear what the cause may be, but possibilities that may merit future study include the following: (a) Conceivably another protein kinase activated during hypertrophy or HF might phosphorylate the same Na^+ channel sites as CaMKII, causing slow open-state I_{Na} inactivation and enhancing late I_{Na}; (b) There could be less local phosphatase at the Na^+ channel in HF (as reported for the ryanodine receptor; refs. 11, 27); (c) Normal cardiac Na^+ channels can also shift into a bursting mode to produce persistent I_{Na} (28, 29), and persistent I_{Na} may have different TTX sensitivity and E_m dependence from transient I_{Na} (30) and contribute to lengthening AP duration in HF (5); (d) Some of the additional Na^+ channels expressed in CaMKIIδ_C-Tg mice (Figure 7G) could be an altered form with weaker inactivation. Regardless of the underlying mechanism, an impaired fast Na^+ channel inactivation mimics the functional defects of mutant Na^+ channels associated with congenital LQT3 (1, 31) and therefore may not only prolong AP and increase $[Na]_i$ but also predispose to VT.

Divergent effects on gating and possible clinical implications for arrhythmias. CaMKIIδ_C enhances steady-state and I_{IM}, while at the same time impairing I_{fast} and enhancing persistent I_{Na}. Strikingly similar changes in Na^+ channel gating were shown for a human mutant Na^+ channel (Asp insertion at 1795 in the C terminus), which shows simultaneous LQT3-like and Brugada-like phenotypes (18). Mutant *1795insD* Na^+ channels expressed in mammalian cells exhibit a shift in steady-state inactivation to negative potentials (with unaltered activation), slowed inactivation, induced persistent I_{Na}, and delayed recovery from inactivation (18, 19). The net effect of both changes would be heart rate dependent. At low frequencies, impaired I_{fast} and persistent I_{Na} outweigh the slowed recovery from inactivation because of long-lasting diastolic intervals. This would favor AP prolongation, consistent with LQT3 syndrome (1) but also HF (4). However, at higher heart rates, there was incomplete I_{Na} recovery, reduced I_{Na} availability, and AP shortening. The consequent loss of Na^+ channel function would then slow propagation and increase dispersion of repolarization. This dual scenario was also demonstrated by computational simulations that incorporate the altered I_{Na} gating properties (32). Similarly, this mixed I_{Na} phenotype was reported in a mutant Na^+ channel (33) with the C terminus truncated at Ser1885 exhibiting negatively shifted steady-state channel inactivation (unchanged activation) and an increase in the fraction of channels that fail to inactivate (slowed inactivation). Therefore, it is conceivable that increased CaMKIIδ_C activity in HF (9, 10) may alter Na^+ channel gating, thereby generating the substrate for VT.

Indeed, CaMKIIδ_C-Tg mice showed an increased propensity for VT in vivo. We show that in CaMKIIδ_C mice, QRS duration was prolonged, indicating slowed intraventricular conduction, which is known to be proarrhythmic in Brugada syndrome. We also show

that repolarization was disturbed in Tg mice, which favors VT in LQT3 patients. MAP duration was significantly prolonged, such that enhanced late I_{Na} with CaMKIIδ_C overexpression could contribute to AP prolongation, EADs, and LQT3-like arrhythmias.

The resulting increased $[Na]_i$ could also drive up SR Ca^{2+} content via Na^+/Ca^{2+} exchange, leading to spontaneous SR Ca^{2+} release and DADs. Interestingly, MAP prolongation was only observed at slower pacing frequencies, indicating heart rate dependence. The CaMKII-dependent I_{Na} modulation reported here may be an acquired form of combined LQT3 and Brugada syndrome, in otherwise normal Na^+ channels. Such an acquired Na^+ channel dysfunction may contribute to arrhythmias under conditions wherein CaMKII effects are enhanced, as in HF (9–11).

While CaMKII-dependent Na^+ channel gating may contribute to the arrhythmias seen in CaMKIIδ_C-Tg mice, changes in other ion channels may certainly also contribute and exacerbate the arrhythmogenic potential of CaMKII-modified Na^+ channels. CaMKII alters L-type Ca^{2+} current and mediates I_{Ca} facilitation, and a reactivation of I_{Ca} during the AP can cause EADs (15, 34). CaMKII-dependent phospholamban phosphorylation also enhances SR Ca^{2+} ATPase activity (12), and the increase in SR Ca^{2+} content would tend to increase spontaneous SR Ca^{2+} release. Additionally, CaMKII-dependent ryanodine receptor phosphorylation increases spontaneous Ca^{2+} release events (12, 13, 35). Both of these SR effects could enhance DADs and trigger arrhythmias independent of Na^+ channel effects. Further studies are required to isolate the relevance of these mechanisms to the arrhythmogenesis in CaMKII-Tg mice.

In summary, our study revealed that CaMKII associates with and phosphorylates cardiac Na^+ channels. CaMKIIδ_C increases steady-state Na^+ channel inactivation through enhanced I_{IM} and slows channel recovery. In contrast, CaMKII also slows open-state inactivation, thereby increasing late I_{Na} and $[Na]_i$. This study characterizes CaMKII effects on Na^+ channel gating that may have important clinical implications for a much larger poluation of patients than those documented to have genetic LQT3 or Brugada syndromes. However, further studies are required, e.g., investigating which Na^+ channel sites associate with and are phosphorylated by CaMKII and precisely how important this pathway (versus others) may be arrhythmogenic in HF.

Methods

CaMKIIδ_C-Tg mice. Tg mice were generated as previously described (12). We used 5.5 ± 0.3–month-old CaMKIIδ_C-Tg mice with HF (12) and age- and sex-matched WT littermates. Ventricular myocytes were isolated (13) and kept in modified Tyrode solution (in mM): 137 NaCl, 5.4 KCl, 1.2 $MgSO_4$, 1.2 Na_2HPO_4, 20 HEPES, 15 glucose, 1 $CaCl_2$ (pH 7.4). All animal studies were approved by the Ethics Committee of the Medical Faculty of the University of Göttingen (Göttingen, Germany).

Adenovirus-mediated CaMKIIδ_C transfection of rabbit myocytes. Ventricular myocytes were isolated from rabbits and plated on culture dishes (36). Transfection with recombinant adenovirus encoding for HA-tagged CaMKIIδ_C (or β-gal as control) was performed at an MOI of 100 during plating of rabbit myocytes in supplemented M199 culture medium for 24 hours (34, 37).

Western blots. Transfected rabbit myocytes were harvested and lysed in Tris buffer (in mM: 20 Tris-HCl, 200 NaCl, 20 NaF, 1 Na_3VO_4, 2% 3-[(3-cholamidopropyl)dimethylammonio]-1-propanesulfonate (CHAPS), 1 DTT [pH 7.4]) and complete protease inhibitor cocktail (Roche Diagnostics) by trituration. Whole mouse hearts were homogenized in Tris buffer. Protein concentration was determined by BCA assay (Pierce Biotechnology). Denatured cell lysates and tissue homogenates (30 minutes, 37°C in 2% β-mercaptoethanol) were subjected to Western blotting (7.5% SDS-polyacrylamide gels) using a rabbit polyclonal anti-Pan Na_v or cardiac-specific anti-$Na_v1.5$ (1:500; Alomone Labs) as primary and an HRP-conjugated donkey anti-rabbit IgG (1:10,000; Amersham Biosciences) as secondary antibody. Chemiluminescent detection was done with SuperSignal West Pico Substrate (Pierce Biotechnology).

Coimmunoprecipitation. Whole mouse hearts were homogenized in Tris buffer (in mM: 50 Tris-HCl, 200 NaCl, 20 NaF, 1 Na_3VO_4, 1 DTT [pH 7.4]) and protease inhibitor cocktail. Protein concentration was determined by BCA assay. Rabbit myocytes were lysed as described above. Mouse homogenates (1 mg protein) and rabbit cell lysates were suspended in dilution medium (in mM: 50 Tris-HCl, 154 NaCl, 1% CHAPS, 1 NaF, 1 Na_3VO_4 [pH 7.4]) and protease inhibitor cocktail. CaMKII was immunoprecipitated with rabbit polyclonal anti-CaMKII antibody (3 μg/mg protein, preincubation at 4°C overnight; M-176; Santa Cruz Biotechnology Inc.) and protein G–sepharose Fast Flow (prewashed; 2 hours, 4°C; Amersham Biosciences). As control, rabbit polyclonal anti-$Ca_v1.2a$ (Alomone Labs) was used. After centrifugation, the pellets were washed with Tris buffer (in mM: 50 Tris-HCl, 154 NaCl [pH 7.4]), and immunoprecipitated proteins were eluted in 2× Laemmli sample buffer containing 4% β-mercaptoethanol (30 minutes, 37°C) followed by centrifugation. Supernatants were subjected to Western blotting.

Immunoprecipitation and back-phosphorylation. Na^+ channels were immunoprecipitated using anti-Pan Na_v (5 μg/mg) and protein G–sepharose (2 hours, 4°C). Immunoprecipitated Na^+ channels were resuspended in 1× CaMKII reaction buffer (in mM): 50 Tris-HCl, 10 $MgCl_2$, 2 dithiothreitol, 0.1 Na_2 EDTA (pH 7.4). CaMKII (30 U) was preactivated (New England Biolabs Inc.) in either the presence or absence of CaMKII inhibitors KN93, AIP, or PKA/PKC inhibitor cocktail (peptide inhibitors of both PKA and PKC; Upstate USA Inc.). Immunoprecipitated proteins were phosphorylated with CaMKII (30 minutes, 30°C) in the presence of ATP-γ-^{32}P with a specific activity of 5.7 Ci/mmol. Beads were washed with RIPA buffer, and proteins were eluted with 2× Laemmli sample buffer containing 4% β-mercaptoethanol (30 minutes, 37°C) followed by centrifugation. Supernatants were separated on SDS–7.5% polyacrylamide gel, and phosphorylated proteins were visualized using a phosphoimager. For some experiments, rabbit myocytes were saponin permeabilized (35). After 5 minutes superfusion with a relaxation buffer containing (in mM) 150 K-aspartate, 0.1 EGTA, 5 ATP, 10 HEPES, 0.25 $MgCl_2$, and 10 reduced glutathione (pH 7.4, 23°C), 50 μg/ml saponin was added for 30 seconds. After permeabilization, myocytes were exposed to internal solution composed of (in mM) 120 K-aspartate, 1 EGTA, 10 HEPES, 5 Na_2ATP, 10 reduced glutathione, 5 U/ml creatine phosphokinase, 10 phosphocreatine, 4% dextran (Mr, 40,000), 5.7 $MgCl_2$ (1 free [Mg]), 0.25 $CaCl_2$ (50 nM free $[Ca^{2+}]$), PKA inhibitory peptide (PKI; 15 μM), pH 7.2. After 5 minutes equilibration, okadaic acid (2 μM) was added to prevent dephosphorylation, and for 5 minutes, free $[Ca^{2+}]$ was either left at 50 nM or raised to 500 nM (plus 2 μM added CaM; Upstate USA Inc.) to activate endogenous CaMKII. Then myocytes were harvested and lysed, and Na^+ channels were immunoprecipitated (dilution medium with 20 mM NaF) and subjected to phosphorylation by exogenous preactivated CaMKII as described above.

Coimmunocytochemical staining. Transfected myocytes were washed (PBS), fixed (4% paraformaldehyde, 30 minutes, room temperature), and blocked with 1% BSA (overnight, 4°C). Cells were incubated with primary antibodies (monoclonal mouse anti-HA, 1:100 [Roche Diagnostics]; rabbit polyclonal anti-$Na_v1.5$, 1:60) in 0.5% BSA and 0.75% Triton X-100 (1 hour, 37°C). After washing (PBS), incubation with secondary antibodies (Texas red–conjugated goat anti-mouse IgG, fluorescein-conjugated goat anti-rabbit IgG, 1:200; Jackson ImmunoResearch Laboratories Inc.) was done in 0.5% BSA (1 hour, 37°C). Cells were covered with VECTASHIELD HardSet Mounting Medium (Vector Laboratories) and viewed using an LSM 5 Pascal confocal microscope (Zeiss). For control, no primary antibodies were used.

Patch-clamp experiments. Ruptured-patch whole-cell voltage-clamp was used to measure I_{Na} with microelectrodes (2–3 MΩ, room temperature). Liquid junction potentials were corrected before GΩ seal establishment. Pipette resistance was compensated in cell-attached configuration. C_m and series resistance (R_s) were compensated automatically (using small negative pulses; where currents were capacitive, they were scaled and subtracted from currents during test pulses), largely eliminating capacitance spikes from the records. C_m and R_s were compensated after patch rupture; access resistance was typically less than 7 MΩ. A continuous R_s compensation was done during measurements (50%). All recordings were done 5 minutes after rupture. Signals were filtered with 2.9- and 10-kHz Bessel filters and recorded with an EPC10 amplifier (HEKA). Pipettes were filled with (in mM) 40 CsCl, 80 Cs-glutamate, 10 NaCl, 0.92 $MgCl_2$, 5 Mg-ATP, 0.3 Li-GTP, 10 HEPES, 0.03 niflumic acid, 0.02 nifedipine, 0.004 strophanthidin, 5 BAPTA (tetracesium salt), 1 5,5′-dibromo BAPTA (tetrapotassium salt), 1.49 $CaCl_2$ (free $[Ca^{2+}]_i$, 100 nM), or 3.73 mM $CaCl_2$ (free $[Ca^{2+}]_i$, 500 nM) (pH 7.2, CsOH).

The bath solution contained (in mM) 10 NaCl, 130 tetramethylammonium chloride, 4 CsCl, 1 $MgCl_2$, 10 glucose, 10 HEPES, 0.0001 thapsigargin (pH 7.4, NaOH). Nifedipine, strophanthidin, and thapsigargin were added to the pipette and bath solution. Low $[Na]_o$ solutions were used for better voltage control. We cannot exclude voltage errors completely, but the I_{Na} amplitudes were similar among groups, so comparisons should still be valid. Some experiments were done in physiologic $[Na]_o$ with bath solution containing 140 mM NaCl without tetramethylammonium chloride. In all experiments, myocytes were mounted on the stage of a microscope (Eclipse TE2000-U; Nikon).

$[Na]_i$. Myocytes were loaded with 10 μM sodium-binding benzofuran isophthalate–AM (SBFI-AM; Invitrogen) for 2 hours at room temperature (36, 38), mounted on the microscope stage, and superfused with Tyrode solution (in mM): 140 NaCl, 4 KCl, 1 $MgCl_2$, 5 HEPES, 10 glucose, 1 (mouse) or 2 (rabbit) $CaCl_2$ (pH 7.4, 37°C). Myocytes were paced at various stimulation frequencies using field stimulation (10–20 V). SBFI was alternately excited (340 and 380 nm), and emitted epifluorescence was monitored at 510 nm (F_{340} and F_{380}) and recorded (IonOptix Corp.). After washout of external dye, background fluorescence was determined. The ratio F_{340}/F_{380} was calculated from the background-subtracted emission intensities and converted to $[Na]_i$. In situ calibration of SBFI was accomplished as described previously (39).

Electrophysiological studies in vivo. Electrophysiological studies in vivo were performed similarly to those in a previously described study (40). Mice were anesthetized with isoflurane and intubated endotracheally. Animals were placed on a thermoregulated table (37°C) and ventilated with isoflurane (2%) vaporized in 100% O_2 using positive pressure ventilation (6 μl/g tidal volume, 140 breaths/min). Subcutaneous 27-gauge needles were placed in all limbs for ECG recordings. Resting ECGs were analyzed for RR interval, heart rate QT_c (41), QRS width, and PR interval. After measurement of resting ECGs, the thorax was carefully entered by an abdominal access through the diaphragm to avoid cardiac injury, and epicardial electrodes were attached to the ventricles. Standard pacing protocols were used to determine electrophysiologic parameters (at twice the diastolic capture threshold). Induction of arrhythmias was attempted using programmed stimulation. Ten spontaneous beats were sensed, followed by 2 consecutive premature beats (S2-S3) at 38-ms intervals. Reproducibly induced VT was defined as 2 consecutive inductions of VT with at least 4 consecutive beats of ventricular origin.

For isoproterenol experiments, animals were anesthetized using 2.5% Avertin, and an equivalent of a lead II recording at 10 kHz was performed. After stabilization of the preparation, a control recording period (2 minutes) was followed by intraperitoneal injection of isoproterenol (2 mg/kg), and ECGs were recorded for an additional 5 minutes.

MAP measurements in the intact, beating heart. MAPs were recorded from right- and left-ventricular epicardium of isolated, Langendorff-perfused hearts as described previously (15, 42). Right-ventricular septal stimulation at fix pacing cycle lengths and S2 extra stimulation for determination of effective refractory periods were performed using an octapolar catheter (CIBER MOUSE; NuMED). Recordings were digitized at 2 KHz and analyzed for MAP duration.

CaMKII inhibitors. KN93 (Seikagaku Corp.) or AIP (Sigma-Aldrich) were added to the pipette solution (final concentration 1 or 0.1 μM, respectively). For back-phosphorylation concentrations in reaction buffer were 50 or 5 μM, respectively. For measurements of $[Na]_i$ and MAP recordings, KN93 (1 μM) was added to the Tyrode solution and perfusate, respectively. Wash-in–washout experiments were performed in the isolated heart.

Statistics. All data are expressed as mean ± SEM. To study I_{fast}, I_{Na} decay (first 50 ms) was fitted with a double exponential function. For late component of I_{Na} decay analysis, recordings at –20 mV (1,000-ms duration) were leakage subtracted using the remaining current after 1,000 ms of depolarization, followed by normalization to peak current. The current integral of the resulting current between 50 and 500 ms was calculated.

Fits were tested for significant difference using *F* tests. For longitudinal data, 2-way repeated-measures ANOVA was run; otherwise, Student's unpaired *t* test was used. For MAP recordings only, Student's paired *t* test was used. Two-sided $P < 0.05$ was considered significant.

Acknowledgments

This work was funded by the Deutsche Forschungsgemeinschaft (DFG) through an Emmy-Noether grant (MA1982/1-4) and Klinische Forschergruppe grant (MA1982/2-1) to L.S. Maier; DFG SFB 656/A5 (to P. Kirchhof) and C3 (to L. Fabritz) and DFG MA2252 (to S.K.G. Maier); Interdisziplinäres Zentrum für Klinische Forschung Münster (ZPG/4a to P. Kirchhof); and NIH grants HL64724 and HL80101 (to D.M. Bers). We acknowledge the technical assistance of A. Steen, G. Müller, M. Kothe, M. Kohlhaas, and E. Hacker.

Received for publication August 18, 2005, and accepted in revised form October 3, 2006.

Address correspondence to: Lars S. Maier, Department of Cardiology and Pneumology, Georg-August-University Göttingen, Robert-Koch-Str. 40, 37075 Göttingen, Germany. Phone: 49-551-399481; Fax: 49-551-398941; E-mail: lmaier@med.uni-goettingen.de.

Nataliya Dybkova and Eva C.L. Rasenack contributed equally to this work.

1. Bennett, P., Yazawa, K., Makita, N., and George, A. 1995. Molecular mechanism for an inherited cardiac arrhythmia. *Nature.* **376**:683–685.
2. Wang, D.W., Makita, N., Kitabatake, A., Balser, J.R., and George, A.L., Jr. 2000. Enhanced Na^+ channel intermediate inactivation in Brugada syndrome. *Circ. Res.* **87**:E37–E43.
3. Bers, D.M. 2001. *Excitation-contraction coupling and cardiac contractile force*. Kluwer Academic Publishers. Dordrecht, The Netherlands. 427 pp.
4. Tomaselli, G.F., and Zipes, D.P. 2004. What causes sudden death in heart failure? *Circ. Res.* **95**:754–763.
5. Undrovinas, A.I., Maltsev, V.A., and Sabbah, H.N. 1999. Repolarization abnormalities in cardiomyocytes of dogs with chronic heart failure: role of sustained inward current. *Cell. Mol. Life Sci.* **55**:494–505.
6. Despa, S., Islam, M.A., Weber, C.R., Pogwizd, S.M., and Bers, D.M. 2002. Intracellular Na^+ concentration is elevated in heart failure but Na/K pump function is unchanged. *Circulation.* **105**:2543–2548.
7. Tan, H., et al. 2002. A calcium sensor in the sodium channel modulates cardiac excitability. *Nature.* **415**:442–447.
8. Maier, L.S., and Bers, D.M. 2002. Calcium, calmodulin, and calcium-calmodulin kinase II: heartbeat to heartbeat and beyond. *J. Mol. Cell. Cardiol.* **34**:919–939.

9. Kirchhefer, U., Schmitz, W., Scholz, H., and Neumann, J. 1999. Activity of cAMP-dependent protein kinase and Ca^{2+}/calmodulin-dependent protein kinase in failing and nonfailing human hearts. *Cardiovasc. Res.* **42**:254–261.
10. Hoch, B., Meyer, R., Hetzer, R., Krause, E.-G., and Karczewski, P. 1999. Identification and expression of δ-isoforms of the multifunctional Ca^{2+}/calmodulin-dependent protein kinase in failing and nonfailing human myocardium. *Circ. Res.* **84**:713–721.
11. Ai, X., Curran, J.W., Shannon, T.R., Bers, D.M., and Pogwizd, S.M. 2005. Ca^{2+}/calmodulin-dependent protein kinase modulates cardiac ryanodine receptor phosphorylation and sarcoplasmic reticulum Ca^{2+} leak in heart failure. *Circ. Res.* **97**:1314–1322.
12. Zhang, T., et al. 2003. The δ_C isoform of CaMKII is activated in cardiac hypertrophy and induces dilated cardiomyopathy and heart failure. *Circ. Res.* **92**:912–919.
13. Maier, L.S., et al. 2003. Transgenic CaMKIIδ_C overexpression uniquely alters cardiac myocyte Ca^{2+} handling: reduced SR Ca^{2+} load and activated SR Ca^{2+} release. *Circ. Res.* **92**:904–911.
14. Zhang, R., et al. 2005. Calmodulin kinase II inhibition protects against structural heart disease. *Nat. Med.* **11**:409–417.
15. Wu, Y., et al. 2002. Calmodulin kinase II and arrhythmias in a mouse model of cardiac hypertrophy. *Circulation.* **106**:1288–1293.
16. Khoo, M.S., et al. 2005. Calmodulin kinase II activity is required for normal atrioventricular nodal conduction. *Heart Rhythm.* **2**:634–640.
17. Koller, B.S., Karasik, P.E., Solomon, A.J., and Franz, M.R. 1995. Relation between repolarization and refractoriness during programmed electrical stimulation in the human right ventricle. Implications for ventricular tachycardia induction. *Circulation.* **91**:2378–2384.
18. Veldkamp, M.W., et al. 2000. Two distinct congenital arrhythmias evoked by a multidysfunctional Na^+ channel. *Circ. Res.* **86**:91e–97e.
19. Bezzina, C., et al. 1999. A single Na^+ channel mutation causing both long-QT and Brugada syndromes. *Circ. Res.* **85**:1206–1213.
20. Wagner, S., and Maier, L.S. 2006. Modulation of cardiac Na^+ and Ca^{2+} currents by CaM and CaMKII. *J. Cardiovasc. Electrophysiol.* **17**(Suppl. 1):S26–S33.
21. Deschênes, I., et al. 2002. Isoform-specific modulation of voltage-gated Na^+ channels by calmodulin. *Circ. Res.* **90**:49e–57e.
22. Kim, J., et al. 2004. Calmodulin mediates Ca^{2+} sensitivity of sodium channels. *J. Biol. Chem.* **279**:45004–45012.
23. Abriel, H., and Kass, R.S. 2005. Regulation of the voltage-gated cardiac sodium channel Nav1.5 by interacting proteins. *Trends Cardiovasc. Med.* **15**:35–40.
24. Kääb, S., et al. 1996. Ionic mechanism of action potential prolongation in ventricular myocytes from dogs with pacing-induced heart failure. *Circ. Res.* **78**:262–273.
25. Pieske, B., et al. 2002. Rate dependence of $[Na^+]_i$ and contractility in nonfailing and failing human myocardium. *Circulation.* **106**:447–453.
26. Attwell, D., Cohen, I., Eisner, D., Ohba, M., and Ojeda, C. 1979. The steady state TTX-sensitive ("window") sodium current in cardiac Purkinje fibres. *Pflügers Arch.* **379**:137–142.
27. Marx, S.O., et al. 2000. PKA phosphorylation dissociates FKBP12.6 from the calcium release channel (ryanodine receptor): defective regulation in failing hearts. *Cell.* **101**:365–376.
28. Maltsev, V.A., et al. 1998. Novel, ultraslow inactivating sodium current in human ventricular cardiomyocytes. *Circulation.* **98**:2545–2552.
29. Nilius, B. 1988. Modal gating behavior of cardiac sodium channels in cell-free membrane patches. *Biophys. J.* **53**:857–862.
30. Saint, D.A., Ju, Y.K., and Gage, P.W. 1992. A persistent sodium current in rat ventricular myocytes. *J. Physiol.* **453**:219–231.
31. Wang, D.W., Yazawa, K., George, A.L., Jr., and Bennett, P.B. 1996. Characterization of human cardiac Na^+ channel mutations in the congenital long QT syndrome. *Proc. Natl. Acad. Sci. U. S. A.* **93**:13200–13205.
32. Clancy, C.E., and Rudy, Y. 2002. Na^+ channel mutation that causes both Brugada and long-QT syndrome phenotypes: a simulation study of mechanism. *Circulation.* **105**:1208–1213.
33. Cormier, J.W., Rivolta, I., Tateyama, M., Yang, A.-S., and Kass, R.S. 2002. Secondary structure of the human cardiac Na^+ channel C terminus. Evidence for a role of helical structures in modulation of channel inactivation. *J. Biol. Chem.* **277**:9233–9241.
34. Kohlhaas, M., et al. 2006. Increased sarcoplasmic reticulum calcium leak but unaltered contractility by acute CaMKII overexpression in isolated rabbit cardiac myocytes. *Circ. Res.* **98**:235–244.
35. Guo, T., Zhang, T., Mestril, R., and Bers, D.M. 2006. Ca^{2+}/Calmodulin-dependent protein kinase II phosphorylation of ryanodine receptor does affect calcium sparks in mouse ventricular myocytes. *Circ. Res.* **99**:398–406.
36. Wagner, S., et al. 2003. Na^+-Ca^{2+} exchanger overexpression predisposes to reactive oxygen species-induced injury. *Cardiovasc. Res.* **60**:404–412.
37. Zhu, W.Z., et al. 2003. Linkage of β_1-adrenergic stimulation to apoptotic heart cell death through protein kinase A-independent activation of Ca^{2+}/calmodulin kinase II. *J. Clin. Invest.* **111**:617–625. doi:10.1172/JCI200316326.
38. Song, Y., Shryock, J.C., Wagner, S., Belardinelli, L., and Maier, L.S. 2006. Blocking late sodium current reduces hydrogen peroxide-induced arrhythmogenic activity and contractile dysfunction. *J. Pharmacol. Exp. Ther.* **318**:214–222.
39. Maier, L.S., Pieske, B., and Allen, D.G. 1997. Influence of stimulation frequency on $[Na^+]_i$ and contractile function in Langendorff-perfused rat heart. *Am. J. Physiol.* **273**:H1246–H1254.
40. Wehrens, X.H., et al. 2004. Protection from cardiac arrhythmia through ryanodine receptor-stabilizing protein calstabin2. *Science.* **304**:292–296.
41. Mitchell, G.F., Jeron, A., and Koren, G. 1998. Measurement of heart rate and Q-T interval in the conscious mouse. *Am. J. Physiol.* **274**:H747–H751.
42. Fabritz, L., et al. 2003. Effect of pacing and mexiletine on action potential duration, dispersion of repolarisation, afterdepolarisations, and ventricular arrhythmias in hearts of SCN5A delta-KPQ (LQT3) mice. *Cardiovasc. Res.* **57**:1085–1093.